

# Phase Space Engineering in Optical Microcavities

## II. Controlling the far-field<sup>1</sup>

Julien Poirier, Guillaume Painchaud-April, Denis Gagnon, Louis J. Dubé<sup>2</sup>

*Département de physique, de génie physique, et d'optique  
Université Laval, Québec, Québec, Canada, G1V 0A6*

### ABSTRACT

Optical microcavities support Whispering Gallery Modes (WGMs) with a very high quality factor  $Q$ . However, WGMs typically display a far-field isotropic emission profile and modifying this far-field profile without spoiling the associated high  $Q$  remains a challenge. Using a 2D annular cavity, we present a procedure capable to achieve these two apparently conflicting goals. With the correspondence between the classical and the wave picture, properties of the classical phase space shed some light on the characteristics of the wave dynamics. Specifically, the annular cavity has a well separated *mixed* phase space, a characteristic that proves to be of crucial importance in the emission properties of WGMs. While the onset of directionality in the far-field may be achieved through parametric deformation [1] of the distance cavity-hole centers,  $d$ , this contribution presents a method to control the emission profile via a second parameter, the hole radius  $r_0$ . The influence of the classical dynamics to *control and predict* the field emission will be demonstrated.

**Keywords:** Optical resonators, annular microcavities, microlasers, whispering-gallery mode, control of directional emission, classical versus wave dynamics

### 1. INTRODUCTION

Whispering Gallery Modes (WGMs) are known to exist in certain types of microcavities. For instance, the class of regularly shaped dielectric structures includes the sphere, the toroid and the disk (thin cylinder) cavities. The strong confinement of the light field, characteristic of the WGMs, appears as sharp peaks of the spectral response of these dielectric microcavities. Accordingly, these cavities possess high quality (high  $Q$ ) modes. Although this property is of central importance for most, if not all, applications of microcavities, the complete uniformity of the emitted far-field distribution of WGMs remains an impediment for useful light source applications (*e.g.* microlasers [2, 3]).

This paper is the sequel of a previous contribution (see [1] in these Proceedings). We will be interested in the parametrical *control* of the far-field patterns of a WGM located inside an annular dielectric cavity. Our approach follows the observation made in [1] that the behavior of the far-field of a WGM may be *triggered* from uniformity to non-uniformity using the center-to-center distance  $d$  (see figure 1(a)). We will exploit the correspondence between the rise of non-uniformity in the far-field distribution (wave picture) and the extent of non-regular dynamics in classical phase space (ray picture) to predict and control the emission.

### 2. CLASSICAL CONCEPTS AND GENERAL CONSIDERATIONS

The geometry of the annular dielectric cavity [4] is depicted in figure 1(a). It consists of an outer disk of radius  $R_0$  and refractive index  $n_C$  in which a circular inclusion of radius  $r_0$  and refractive index  $n_h$  is embedded and whose center is a distance  $d$  from the center of the main disk. The cavity is surrounded by a dielectric medium of index  $n_o$ . In the classical limit, the dynamics within the cavity amounts to follow individual rays as they propagate freely in between collisions with the outer boundary and the inclusion. For an ensemble of many trajectories, the phase space is constructed from the successive coordinates  $\{s_i, p_i\}$  (figure 1(b)) recorded on the surface of the outermost boundary:  $\{s_i\}$  are the arc length and  $\{p_i = \sin \chi_i\}$  where  $\chi_i$  is the angle incidence with respect to the normal. Note that the rays are specularly reflected at the outermost boundary whereas we allow transmission ( $|p| < n_h/n_C$ ) or reflection ( $|p| > n_h/n_C$ ) at the inclusion interfaces. The result is displayed in figure (1(c)). Several features are worth mentioning, some of them unique to the annular cavity.

<sup>1</sup>This research has been funded in part by a Strategic Grant from NSERC (Canada) and a Team Project from FQRNT (Québec).

<sup>2</sup>Corresponding author: ljd@phy.ulaval.ca

The system under study possess a *mixed* dynamics. Even more, phase space is well divided into *two* principal regions: a *regular* domain,  $|p| > p_{\text{NR}} \equiv (d + r_0)/R_0$ , filled with trajectories, reminiscent of the integrable disk dynamics, oblivious to the inclusion, and a *non-regular* domain,  $|p| < p_{\text{NR}}$  where irregular, mostly chaotic, trajectories are observed. The extent of the region where the dynamics is non-regular is simply governed by the position  $d$  and size  $r_0$  of the inclusion and proportional to  $d+r_0$ . Another domain of

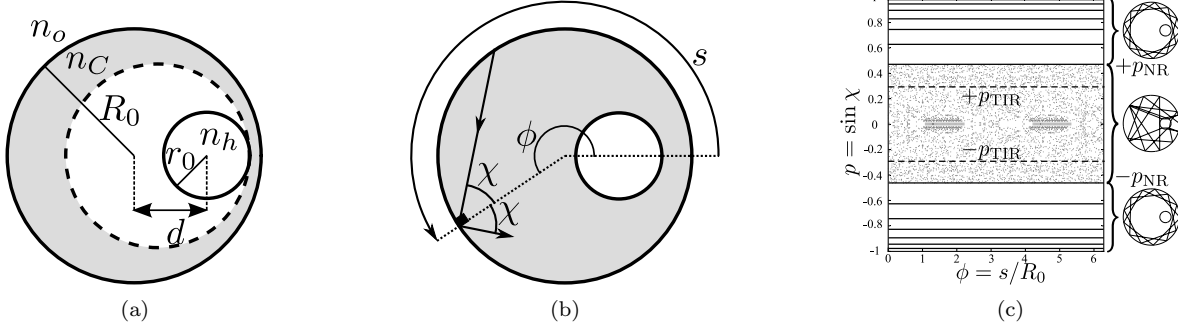


**Figure 1: Geometry and phase space of the annular cavity.** (a) A circular inclusion of refractive index  $n_h$  and radius  $r_0$  is placed a distance  $d$  from the geometrical center of the cavity. The distance of the inclusion  $R_0 - (d + r_0)$  to the boundary will be kept constant in the following; (b) Classical phase space coordinates, arc length  $s$  (alternatively angular position  $\phi = s/R_0$ ) and  $p = \sin \chi$ ; (c) Phase space constructed from the impact coordinates  $\{\phi_i, p_i\}$  for different initial conditions. Two distinct regions, containing regular and irregular trajectories respectively, are apparent and well separated by the geometrical condition  $|p| = p_{\text{NR}} = (d + r_0)/R_0$ . The boundary of a TIR region ( $|p| > p_{\text{TIR}} \sim 0.3$ ) is also indicated.

interest is the classical *emission* (or escape) region defined by the  $E = \{(s, p) : 0 \leq s \leq 2\pi R_0, |p| \leq p_{\text{TIR}}\}$ , under the Snell-Descartes condition of Total Internal Reflexion (TIR) at the outer boundary

$$p_{\text{TIR}} = n_o/n_C \quad . \quad (1)$$

Clearly for  $p_{\text{NR}} > p_{\text{TIR}}$ , the classical far-field emission is strictly determined by the non-regular “chaotic” trajectories [1]. Moreover, only a small subset of  $E$  is actually accessible for emission, we call this subset the *effective* emission region, and denoted it by  $W$ . It consists of the trajectories initially located outside of  $E$  that get mapped to  $E$  through a single iteration of the (implicit) Poincaré map,  $\mathcal{P} : (s_i, p_i) \mapsto (s_{i+1}, p_{i+1})$ . The region  $W$  is then defined as

$$W = \mathcal{P}(\mathcal{P}^{-1}(E) \cap \bar{E}) \quad (2)$$

with the complement  $\bar{E} = \{(s, p) : 0 \leq s \leq 2\pi R_0, p_{\text{TIR}} \leq |p| < 1\}$ . Trajectories entering  $E$  are thereafter bound to escape the cavity. The dynamical system so-defined does not conserve energy (*i.e.* the total amount of initial conditions (or initial intensity) decreases as the trajectories reach  $E$ ).

The domain  $W$  is obviously modified by parametric variations of both  $d$  and  $r_0$ . Since we have observed that the far-field emission of a WGM becomes *non-uniform* with increasing  $d$  (for fixed  $r_0$ ) [1, 5], and accordingly increasing  $p_{\text{NR}}$ , we propose that the *directionality* of the emission may be further engineered by keeping  $d + r_0$  ( $p_{\text{NR}}$ ) constant and changing  $r_0$ , thereby modifying the “mixing” properties of the non-regular region without affecting its size. The quantitative modifications induced will now be investigated in the wave dynamics under the guidance of the previous classical considerations.

### 3. EFFECT OF PARAMETER $r_0$ ON THE FAR-FIELD BEHAVIOR

We approximate our physical annular cavity by a planar (2D) system and search for resonant modes (here TM polarization) by solving Helmholtz equation

$$[\nabla^2 + n^2(r, \phi)k^2] \psi(r, \phi) = 0 \quad (3)$$

under appropriate boundary conditions. The solutions are obtained by a careful implementation of the scattering formalism of [6]. The physical parameters of the system are set as  $n_C = 3.2$ ,  $n_h = n_o = 1$ ,

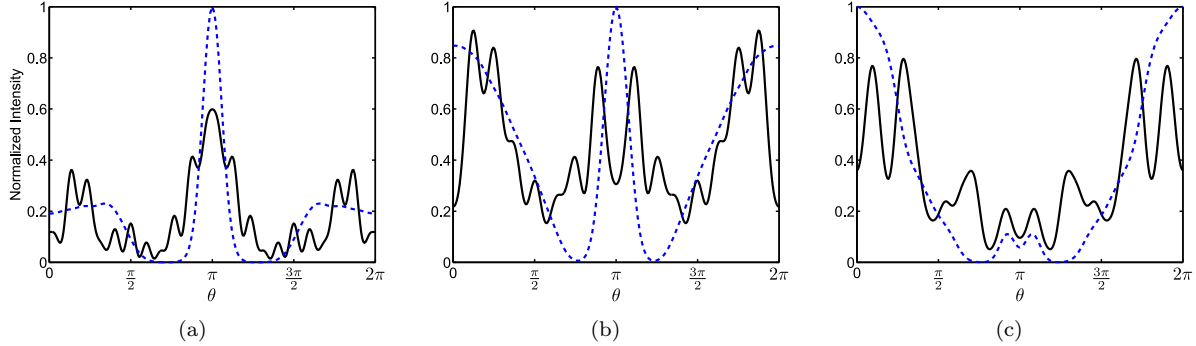


**Figure 2: Far-field intensities.** *full curves: combined envelope of the two symmetries of mode (11, 1),  $|\psi_{(11,1)}^e|^2 + |\psi_{(11,1)}^o|^2$ ; dashed curves: non-coherent sum of the classical trajectories reaching the far-field for 3 values of  $r_0$ , (a)  $r_0 = 0.064R_0$ , (b)  $r_0 = 0.127R_0$ , (c)  $r_0 = 0.211R_0$ , while  $d + r_0$  is kept fixed at  $0.55R_0$ . For ease of comparison, the intensities in each panel have been arbitrarily normalized to the maximum of the classical intensities.*

$R_0 = 1$  keeping the control group  $d + r_0$  constant at  $= 0.55 R_0$ . The important regions are then delimited by  $p_{\text{TIR}} = 0.3125$  and  $p_{\text{NR}} = 0.55$ . For the sake of demonstration, we have selected the high  $Q$  WGM (11, 1) at  $kR_0 \approx 4.5$ . The notation  $(m, n)$  is meant to identify the angular momentum number and the number of radial nodes respectively, and  $k$  is the wavenumber. The particular choice of  $d + r_0$  is motivated by the high far-field contrast value  $C_{11}$  for  $r_0 = 0.20R_0$  and  $d = 0.35R_0$  [1]. This contrast measure  $C_{m_0}$  varies between 0 and 1: 0 meaning that the observed far-field has fully retained its original uniform  $m_0$  character, and 1 indicating that the perturbed mode has mixed with other angular momentum components and that its field distribution is highly non-uniform. We have retained the two symmetries of mode (11, 1) in the full-wave calculations (even/odd,  $\psi_{(11,1)}^{e/o}$ , relative to the center-to-center axis).

We follow the mode (11, 1) as  $r_0$  is varied from  $0.05R_0$  to  $0.40R_0$  and although its quality factor drops from about  $10^7$  to roughly  $10^5$  over the interval, it remains the dominant resonance, albeit with a changing character. The far-field emission is recorded as a function of the observation angle  $\theta$  from the non-coherent sum of  $|\psi_{(11,1)}^e|^2$  and  $|\psi_{(11,1)}^o|^2$ . The far-field intensities are displayed in figure (2) for 3 separate values of  $r_0$ . The emission profiles evolve from a sharp contribution near  $\theta = \pi$  at  $r_0 = 0.064R_0$  (figure 2(a)) to an increasingly broad multi-peaks envelope with equally important contributions around  $\theta = \pi/4, \pi$  and  $3\pi/4$  at  $r_0 = 0.127R_0$  (figure 2(b)) and to a depleted emission in the backward direction in favor of two important forward peaks at  $r_0 = 0.211R_0$  (figure 2(c)). In short, the objective of modifying the directionality of the far-field emission of a WGM through parametric control is achieved.

To connect with the intuition gained in the previous section, we have carried out a ray-escape simulation [7] in the classical representation. Assuming that the transition probability to the effective escape region  $W$  is highest near the  $p_{\text{NR}}$  limit, initial conditions are chosen uniformly in a thin strip of phase space with  $p \sim p_{\text{NR}}$ . For a given  $r_0$ , each initial condition  $(s_0, p_0)$  is followed through consecutive impacts  $(s_i, p_i)$  with the outer boundary where a reflected intensity  $I_{i+1} = I_i(1 - |T(p_{i+1})|^2)$  is calculated with Fresnel transmission coefficient,

$$T(p) = \frac{\sqrt{1 - p^2}}{\sqrt{1 - p^2} + \sqrt{(n_o/n_C)^2 - p^2}}. \quad (4)$$

Iterations stop when the intensity associated with a trajectory has dropped from its initial value  $I_0$  to an arbitrarily small number. The escaping intensities of every trajectory are then binned according to observation angles  $\theta$  to form the far-field distribution. Finally, the classical far-field is convoluted with a gaussian function of width  $\sigma = 2\pi/4m_0$  to smooth out irregularities. The width is chosen to account for the angular resolution of the pure WGM  $(m_0, n)$  which has  $2m_0$  lobes in the azimuthal direction.

The comparison with the full-wave far-field profiles is presented in figure 2. At this low value of  $n_C k R_0 \sim 15$ , it is no surprise that the agreement is only qualitative although the main features are present in both calculations. Our exploratory simulations are nevertheless encouraging and we expect

the procedure to deliver better correspondence at higher values of  $n_C k R_0$ . One should stress however that the classical approach is universal and generic. In the annular geometry studied here, a large number of high  $Q$  WGM ( $m, n$ ) are available above  $|p| = p_{NR}$  and they are well localized around their resonance condition  $p_{WGM} = m/(n_C k R_0)$ . As long as  $p_{WGM} > p_{NR}$ , they are candidate for far-field directionality while preserving their near-field uniformity, i.e. low-loss, high  $Q$  character, and phase space design is a possible route to optimization.

Figure (3) gives a sense of the range of values of the control parameters where one can modify (engineer)

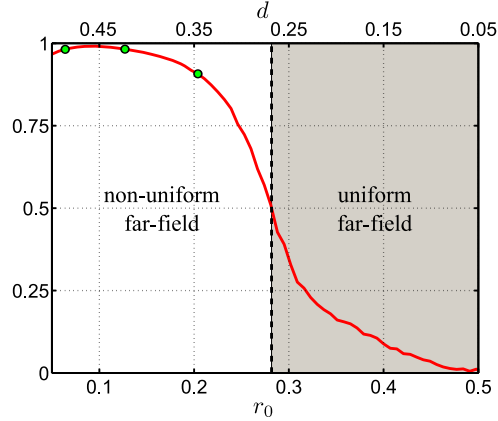


Figure 3: **Constrat measure  $C_{11}$  versus  $r_0$ .** For fixed  $d+r_0 = 0.55$  (distances in unit of  $R_0$ ), 2 regions, non-uniform and uniform far-field, arbitrarily divided at  $C_{11} = 0.5$ , define the range of  $r_0$  for which the far-field profile has a certain character. The 3 dots correspond to the same values of  $r_0$  presented in figure (2).

at will the far-field distribution keeping a high quality factor. The contrast measure  $C_{11}(r_0)$  stays above 0.80, meaning strong mixing with other angular components  $m \neq m_0$ , for  $r_0 \in [\sim 0, \sim 0.25]$ . As  $r_0$  is further increased,  $C_{11}$  drops further until it reaches low values where the WGM has recovered its regular uniform character.

#### 4. CONCLUSION

In this paper we have shown that it is possible to control the directionality of the far-field emission through the modification of the radius  $r_0$  of a circular inclusion in a annular dielectric cavity. Evidences have been presented that the far-field profile of both full-wave and classical simulations show similar structures. Furthermore, for a given annular geometry, the classical far-field profile is universal. Our results along with those of [1, 5] pave the way to design scenarios for high  $Q$  directional emission from WGMs of disk-shaped microcavities.

## REFERENCES

- [1] G. Painchaud-April, J. Poirier, D. Gagnon, and L. J. Dubé: Phase space engineering in optical microcavities I: Preserving near-field uniformity while inducing far-field directionality, in *Proceedings ICTON 2010*, Munich, Germany, July 2010.
- [2] J. U. Nöckel and R. K. Chang: 2D microcavities: theory and experiment, in *Cavity-enhanced spectroscopies* (R. D. van Zee and J. P. Looney, eds.), pp. 185–226, San Diego: Academic Press, 2002.
- [3] K. J. Vahala: Optical microcavities, *Nature*, vol. 424, pp. 839–846, 2003.
- [4] M. Hentschel and K. Richter: Quantum chaos in optical systems: The annular billiard, *Phys. Rev. E*, vol. 66, pp. 056207 (1-13), 2002.
- [5] G. Painchaud-April, J. Poirier, and L. J. Dubé: Competition of escape mechanisms in an optical annular cavity, submitted to *Phys. Rev. E*. (2010).
- [6] A. I. Rahachou and I. V. Zozoulenko: Scattering matrix approach to the resonant states and  $Q$  values of microdisk lasing cavities, *Appl. Opt.*, vol. 43, pp. 1761–1772, 2004.
- [7] H. G. L. Schwefel, N. B. Rex, E. Tureci, R. K. Chang, A. D. Stone, T. Ben-Messaoud and J. Zyss: Dramatic shape sensitivity of directional emission patterns from similarly deformed cylindrical polymer lasers, *J. Opt. Soc. Am. B*, vol. 21, pp. 923–934, 2004.